Deep Resources Engineering 3 (2026) 100236

Contents lists available at ScienceDirect

Deep Resources Engineering

journal homepage: www.keaipublishing.com/en/journals/deepre/

Full length article

Numerical and experimental studies of the natural mixing behavior between an uncemented paste backfill and dumped waste rock in stopes from laboratory toward field conditions. Part II: Application and prediction of the validated and calibrated numerical model

Yuyu Zhang [a], Li Li [a,*], Louis-Philippe Gélinas [b], Serge Ouellet [c]

[a] Research Institute of Mines and Environment (RIME UQAT-Polytechnique), Department of Civil, Geological and Mining Engineering, Polytechnique Montréal, Montréal, QC H3C 3A7, Canada
[b] Agnico Eagle Mines Limited – CSD, Rouyn, Noranda, QC J0Y 1C0, Canada
[c] Agnico Eagle Mines Limited, Malartic, QC J0Y 1Z0, Canada

A R T I C L E I N F O

Keywords:
Waste rocks
Paste backfill
Maximum particle size
Natural mixing behavior
Numerical modeling
Size effects

A B S T R A C T

Directly dumping waste rocks (*WR*) underground produced into mine stopes being filled with cemented paste backfill offers several advantages. However, this practice can also present certain risks, especially when the dumping operation is poorly controlled or when the cohesionless *WR* are not fully or properly mixed with the paste backfill. Therefore, it is critical to understand and well quantify the mixing degree between dumped *WR* and paste backfill in stopes. To date, however, publications addressing the natural mixing behavior between dumped *WR* and paste backfill in stopes are almost nonexistent. Moreover, conducting laboratory tests with oversized *WR* is impractical. Scaling down techniques must be applied to exclude large and oversized particles found in in situ *WR*. Experimental results obtained using *WR* samples with different maximum particle sizes (d_{max}) can then be used to calibrate and validate a numerical model. Once validated and calibrated, the numerical model can be used to evaluate and quantify the mixing degree between dumped *WR* and paste backfill, while accounting for the size effects of both stopes and *WR* particles. In this study, a series of laboratory tests were conducted at different scales, varying both the stope size and the particle size of the *WR*. The validated and calibrated numerical model, presented in the companion paper (Part I), was then applied to predict the experimental results. The model's reliability is partly confirmed by strong agreement between some numerical prediction and experimental results. Consequently, the validated model can be further applied to simulate the natural mixing behavior of a paste backfill and dumped *WR* with larger d_{max} in large-scale scenarios. However, some discrepancies were also observed between certain numerical predictions and test results. These inconsistencies helped identify limitations in both the laboratory testing setup and numerical model itself. As a result, clear directions for future improvements have been established. This study demonstrates the value and potential of numerical modeling as a powerful tool for analyzing the natural mixing behavior in mine backfilling operations.

1. Introduction

Underground mines generate large quantities of waste rock (*WR*) to access ore. Traditionally, most of this *WR* must be hoisted to the surface for disposal in *WR* piles, due to the limited storage space available underground. This transportation process involves substantial energy consumption and additional operational costs, especially with deep mines.

An alternative practice, commonly adopted in many underground mines in Canada (and likely in other countries), is to directly dump the *WR* into stopes that are being filled with cemented paste backfill (PB). This approach significantly reduces the volume of *WR* that must be

* Corresponding author.
E-mail addresses: yuyu.zhang@polymtl.ca (Y. Zhang), li.li@polymtl.ca (L. Li), Louis-Philippe.Gelinas@agnicoeagle.com (L.-P. Gélinas), serge.ouellet@agnicoeagle.com (S. Ouellet).

https://doi.org/10.1016/j.deepre.2026.100236
Received 9 June 2025; Received in revised form 7 January 2026; Accepted 12 January 2026
Available online 19 January 2026

transported over long distance and hoisted to the surface, thereby lowering energy use and operational costs [1]. Moreover, a well-mixed combination of W*R* and cemented PB can exhibit superior mechanical strength compared to either material alone [2–4]. As a result, backfilling costs can be reduced by lowering the required amounts of binder to achieve the same overall required strength.

Despite these numerous advantages, very few studies in the literature have addressed the natural mixing behavior between dumped W*R* and PB. This lack of research is likely due to the complexity and high uncertainty involved in quantifying such mixing behavior. Consequently, mining and backfill engineers are often forced to reply on trial and error approaches. If the dumping of W*R* into stopes being filled with cemented backfill is not properly managed, serious issues can arise, including excessive ore dilution, ore loss, or even collapse of fill mass. When excessive amounts of cohesionless W*R* are dumped, poor or incomplete mixing with the PB may occur. This can result in weak zones or internal structures within the fill mass that may fail upon exposure, either from the side or base, during subsequent excavation.

Understanding the natural mixing behavior between dumped W*R* and PB is therefore critical for ensuring safe and efficient mine operations.

To date, most studies on mining backfills have focused on a single material type, such as hydraulic fill, PB, or rockfill (e.g., [5–23]). Only a few studies have examined mechanically mixed materials such as graded W*R* and tailings slurry, prepared using dedicated equipment [6,24–27]. However, these mixtures require additional equipment, energy, and cost, making them fundamentally different from the naturally formed mixtures created by dumping W*R* into PB.

As such, research focused specifically on the natural mixing behavior of dumped W*R* and PB is urgently needed.

Recently, Zhang and Li [28] conducted a laboratory study on this topic. Their preliminary findings revealed that the degree of mixing between the two materials is influenced by several factors, including the solids content of the PB, the size of the W*R* particles, and the dumping height. Effective mixing was observed when the PB had a low solids content, the W*R* particles were large, and the dumping height was high. In contrast, poor mixing occurred when the PB was too thick or when excessive W*R* was dumped at once. This study provides valuable insights into natural mixing behavior under small-scale laboratory conditions.

While further laboratory tests using larger containers and coarser W*R* are possible, full-scale field testing remains impractical. Therefore, numerical modeling is necessary. However, to build public's and industry confidence, it is essential to ensure the stability, reliability, and representativeness of both the numerical models and the experimental results, as demonstrated in Li [29] and Zhang and Li [30,31].

Part I of this study, presented in the companion paper, demonstrates how to obtain reliable numerical results using an optimal and calibrated numerical model. The importance of clearly distinguishing between calibration and prediction processes is also emphasized. The effects of W*R* particle size on geotechnical behavior are addressed both in the experimental work through sample preparation using the scalping-down technique [32] and in the numerical model by incorporating a rolling resistance coefficient as a function of the maximum particle sizes of the W*R* (d_{max}). Good agreement was achieved between the measured repose angles and the numerical predictions using the validated and calibrated model. These results confirm that the model can be used to analyze the geotechnical behavior of various infrastructures composed of W*R* with particles of any sizes.

However, to simulate the mixing behavior between dumped W*R* and PB, it is necessary to combine the validated and calibrated numerical model for W*R* presented in Part I with the corresponding model for PB developed by Zhang and Li [30].

In this paper, a series of laboratory tests were conducted to evaluate the natural mixing behavior between dumped W*R* and PB, using W*R* samples with varying d_{max} values and different mold sizes. The experimental results are presented, and the numerical models from the companion paper (Part I) and Zhang and Li [30] are applied to predict the outcomes under various testing conditions. If successful, the validated model can then be used to simulate and predict the natural mixing behavior of these two materials at various scales and under both laboratory and field conditions.

2. Laboratory tests on dumping W*R* onto PB

2.1. Tested materials

The W*R* samples used in this study are the same as those for repose angle tests presented in the companion paper (Part I). A scalping-down technique was applied to produce W*R* samples with maximum particle size (d_{max}) values of 2.0, 5.0, and 50.0 mm, respectively. The corresponding masses of the scalped sample were 400, 1400 and 4441 g. Fig. 1 shows their texture (Fig. 1a) and their particle size distribution (PSD) curves (Fig. 1b). To facilitate the numerical modeling, particles smaller than 1.18 mm were excluded from all samples.

The tailings used in this study were collected from the same mine as the W*R* samples. The PSD curve is shown in Fig. 2. The tailings have a d_{max} of 0.63 mm, with approximately 77% of the particles smaller than 80 μm and 36% smaller than 20 μm.

The backfill produced from these tailings meets the PSD criterion of PB, which typically requires at least 15% of particle smaller than 20 μm [6,28]. In this study, the PB was prepared at a solids content of 75% by mass. A photo of the prepared PB is shown in Fig. 3.

2.2. Test procedure

In this study, two sets of mixing tests were conducted. The first set involved scalped waste samples with d_{max} of 2.0 and 5.0 mm, and corresponding masses of 400 and 1400 g, respectively. Fig. 4 shows a schematic diagram (Fig. 4a) and a photograph (Fig. 4b) of the experimental setup. A wooden box measuring 16.5 cm × 20 cm × 25 cm ($L \times W \times H$) was used to simulate an underground mine stope (Fig. 4b). PB was first poured into the box to a height of 10 cm. Next, a specified amount of W*R* was poured into the PB using a funnel positioned at the midpoint of the long side of the mold. The dumping height H_F, measured from the bottom of the funnel to the surface of the PB, was set at 40 cm.

After allowing the mixture to cure for two weeks, the base-undrained mold was carefully disassembled. The hardened sample was then cut. For the test using W*R* with a d_{max} of 2.0 mm, sieving was made to separate the W*R* from the mixture and determine the mass of mixed W*R*. The unmixed mass of W*R* was calculated by subtracting the mixed mass from the total sample mass. For the test using W*R* with a d_{max} of 5.0 mm, the unmixed W*R* was visually separated from the mixture. The unmixed W*R* was then collected and weighed, and the mixed mass was obtained by subtracting the unmixed mass from the total mass.

The second set of tests was conducted using a W*R* sample with a d_{max} of 50 mm. A photograph of the large-scale test model is shown in Fig. 5. A wooden box measuring 36 cm in length, 36 cm in width, and 20 cm in height was used to simulate a larger underground mine stope. PB was first poured into the mold to a height of 15 cm. Then, a total mass of 4441 g of the W*R* was dumped onto the PB via a wooden incline positioned at the center of the mold. The dumping height measured from the bottom of the incline to the surface of the PB was 75 cm.

The dumping was carried out by quickly rotating the wooden incline into a vertical position. To minimize premature dropping of particles

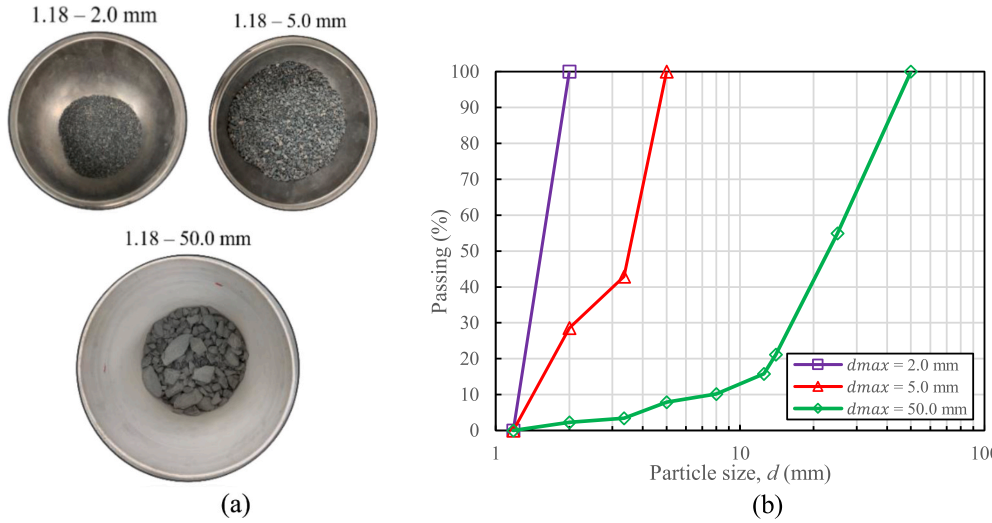

Fig. 1. Scalped *WR* samples with d_{max} of 50.0, 5.0, and 2.0 mm, respectively: (a) a picture of the samples; (b) PSD curves.

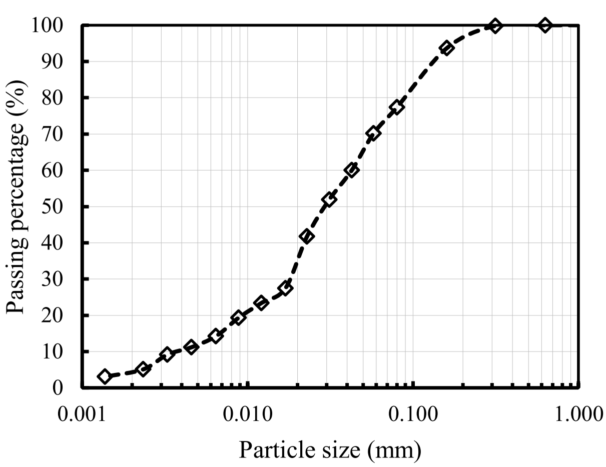

Fig. 2. PSD curve of the tested tailings.

Fig. 3. A photo of tested PB at a solids content of 75% by mass.

during this operation, the bottom of the incline was manually held to control the release of the *WR*. After a curing period of three weeks, once the mixture had hardened sufficiently, the specimen was exposed. The unmixed *WR* was visually separated from the mixture. The unmixed *WR* was then collected and weighed, and the mixed mass was obtained by subtracting the unmixed mass from the total mass.

2.3. Test results

Fig. 6 presents a top view (Fig. 6a) and a side front view without any cut (Fig. 6b) of the mixture formed by dumping *WR* with a d_{max} of 2.0 mm and a total mass of 400 g onto PB, with a dumping height H_F of 40 cm. The scales are added according to the box sizes shown in Fig. 4. It can be seen that a significant portion of the *WR* remains on the top surface of the PB. This is attributed to the combined effects of the high solids content of the PB and the small sizes of *WR* particles. The impact energy of the particles is low, while the drag resistance exerted by the PB against the penetration of the *WR* is high [28]. These factors result in limited mixing, with 364.7 g of *WR* remaining unmixed on the surface and only 35.3 g incorporated into the PB, as determined after cutting the sample.

Fig. 7 presents a top view (Fig. 7a) and a side front view without any cut (Fig. 7b) of the mixture formed by dumping *WR* with a d_{max} of 5.0 mm and a total mass of 1400 g onto PB, from a dumping height H_F of 40 cm. The scales are added according to the box sizes shown in Fig. 4. From the top view (Fig. 7a), a substantial amount of *WR* can be seen remaining on the surface of the PB. The front view (Fig. 7b) further confirms the absence of visible mixing between the dumped *WR* and the PB.

The mass of *WR* that remained unmixed with the PB was measured at 1207 g, indicating that only 193 g of *WR* was incorporated into the PB. These results suggest that the PB, with a solids content of 75%, is likely too thick to allow effective mixing with the tested *WR* particle sizes.

Fig. 8 presents a top view (Fig. 8a) and a cut view (Fig. 8b) of the mixture formed by dumping *WR* with a d_{max} of 50.0 mm and a total mass of 4441 g onto PB from a dumping height H_F of 75 cm. The scales are added according to the box sizes shown in Fig. 5. Both views show that only a small portion of the *WR* remained on the top surface of the PB, while the majority penetrated into the PB.

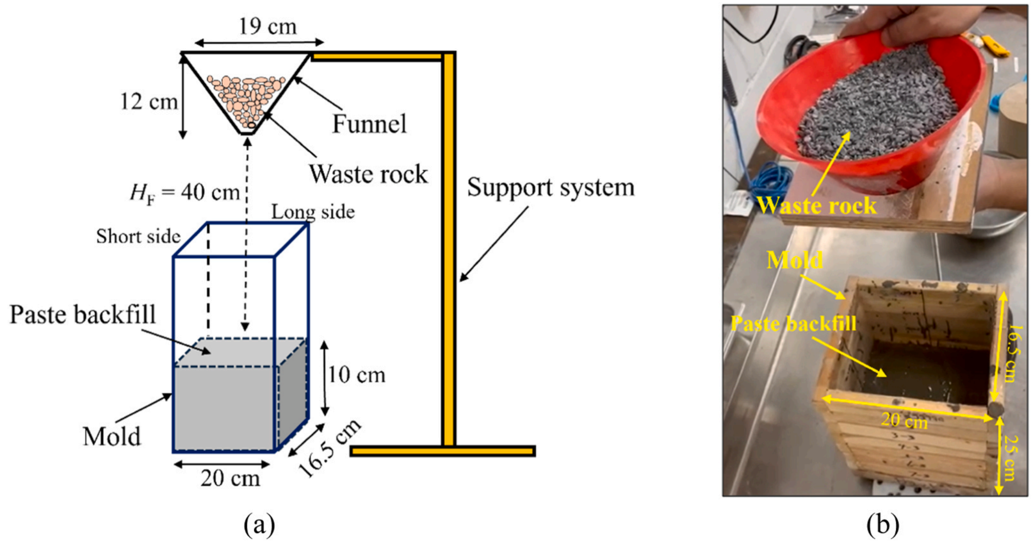

Fig. 4. Small-scale test of pouring *WR* samples onto the PB at a dumping height of 40 cm: (a) schematic presentation; (b) a photo.

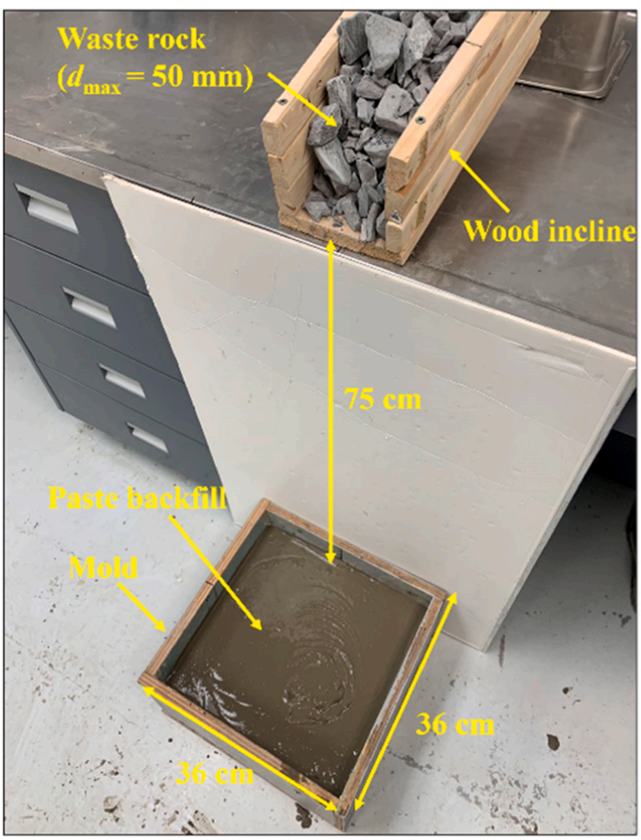

Fig. 5. A photo of the large-scale test by pouring *WR* with d_{max} of 50.0 mm and a total mass of 4441 g onto the PB at a dumping height of 75 cm.

These results differ significantly from those obtained using *WR* samples with d_{max} values of 2.0 and 5.0 mm. The improved mixing is likely due to the combined effects of the larger particle size and greater dumping height. Larger *WR* particles, when dropped from a higher elevation, generate greater impact energy, which enhances their ability to penetrate the PB.

The mass of *WR* that remained unmixed with the PB was measured at 444.5 g, indicating that 3996.5 g was incorporated into the PB.

3. Reproduction of the experimental results by numerical prediction

To numerically predict the experimental results of *WR* dumping into PB, the EDEM software [33] developed on discrete element method was employed. The validation of this numerical model against analytical solutions, ensuring stable and reliable numerical results, has been previously demonstrated in Zhang and Li [30]. Model calibration and validation against laboratory-scale experimental results for the *WR* are detailed in the companion paper (Part I), while the model calibration and validation against laboratory-scale experimental results for the PB was presented in Zhang and Li [30]. The fully validated and calibrated model can be directly applied to simulate and predict the natural mixing behavior between dumped *WR* and PB.

Table 1 summarizes the material parameters used for both *WR* and PB. The parameters for the *WR* are identical to those reported in the Part I. For the PB, the yield stress was determined through slump tests, while the viscosity was obtained via numerical calibration based on steel ball drop tests in PB, as described in Zhang and Li [30].

Fig. 9 presents the numerical model developed in EDEM to simulate the laboratory test in which 400 g of *WR* with a d_{max} of 2.0 mm was poured onto PB from a dumping height of 40 cm. *WR* particles were generated within the funnel using the EDEM Dynamic Factory tool (Fig. 9a). Subsequently, the particles were released from the funnel and allowed to fall onto the PB (Fig. 9b).

The simulation employed the material parameters listed in Table 1. A time step of 1.24×10^{-5} s was used, based on prior time step sensitivity analyses to ensure numerical reliability and computational efficiency.

Fig. 10 presents the mixing state between the dumped *WR* and PB as predicted by the numerical model. For comparison, the corresponding experimental results are also included in the figure. The simulation outcome closely resembles the laboratory observation in terms of the overall distribution and behavior of the materials.

The numerical prediction indicates that 59.46 g of *WR* was mixed with the PB, while 340.54 g remained unmixed. The predicted mass of unmixed *WR* is in good agreement with the measured value of 364.7 g. However, the predicted mass of mixed *WR* is somewhat higher than the experimental measurement of 35.3 g. Despite this discrepancy, the numerical model successfully captures the general mixing behavior observed in the test.

Fig. 11 presents the numerical model developed in EDEM to simulate the laboratory test in which 1400 g of *WR* with a d_{max} of 5.0 mm was poured onto PB from a dumping height of 40 cm. As in the previous case,

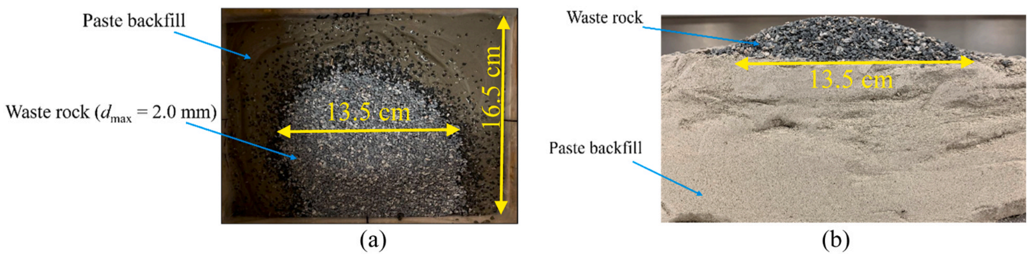

Fig. 6. A top view (a) and a side front view without any cut (b) of the mixing state of the dumped *WR* with a d_{max} of 2.0 mm and a total mass of 400 g onto the PB at a dumping height of 40 cm.

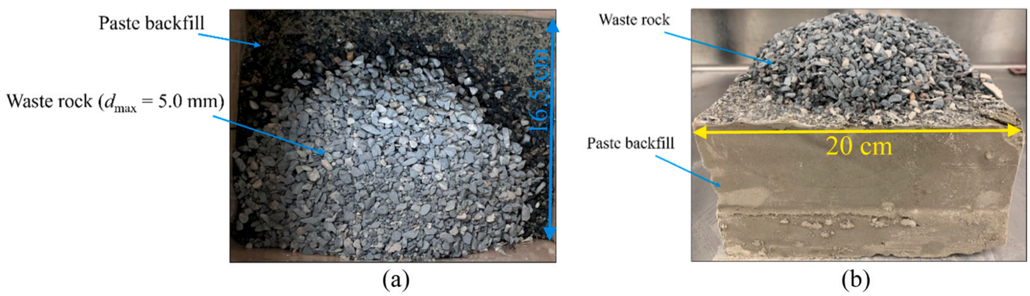

Fig. 7. A top view (a) and a side front view without any cut (b) of the mixing state of the dumped *WR* with a d_{max} of 5.0 mm and a total mass of 1400 g onto the PB at a dumping height of 40 cm.

the *WR* particles were generated within the funnel using the EDEM Dynamic Factory tool (Fig. 11a). They were then released from the funnel to fall freely onto the PB surface (Fig. 11b).

The simulation was conducted using the material parameters listed in Table 1. An optimal time step of 4.96×10^{-6} s, determined through time step sensitivity analyses, was adopted to ensure numerical reliability and computational efficiency.

Fig. 12 shows the mixing state between the dumped *WR* and PB as predicted by the numerical model. The corresponding experimental results are also included for comparison. Once again, the numerical simulation yields a mixing pattern that closely resembles the laboratory observations.

According to the numerical prediction, 131.08 g of *WR* was mixed with the PB, while 1268.9 g of *WR* remained unmixed. These values are reasonably close to the experimentally measured masses of 193 (mixed) and 1207 g (unmixed), respectively. The consistency between the numerical and experimental results further supports the reliability and predictive capacity of the numerical model.

Fig. 13 presents the numerical model developed in EDEM to simulate the large-scale laboratory test, in which 4441 g of WR with a d_{max} of 50.0 mm was poured onto PB from a dumping height of 75 cm. The *WR* particles were generated inside the funnel using the EDEM Dynamic Factory tool and then released from the funnel to fall freely onto the PB surface from the specified height.

Fig. 14 presents the mixing state between the dumped *WR* and PB as obtained from the numerical simulation, alongside the corresponding experimental results. Once again, the numerical model produces a mixing outcome that is generally consistent with the laboratory observations.

The numerical prediction indicates that 3537.66 g of *WR* mixed with the PB, while 903.34 g of *WR* remained unmixed. The predicted mixed mass is reasonably close to the measured value of 3996.5 g. However, the predicted unmixed mass is notably higher than the experimental measurement of 444.5 g.

Table 2 summarizes the measured and numerically predicted masses of mixed and unmixed *WR* in PB for all test cases. The results show that the validated and calibrated numerical model can quantitatively predict the mixing behavior of dumped *WR* and PB with reasonable accuracy in some cases, though not all. The source of these discrepancies and heir implication will be discussed further in Section 4.

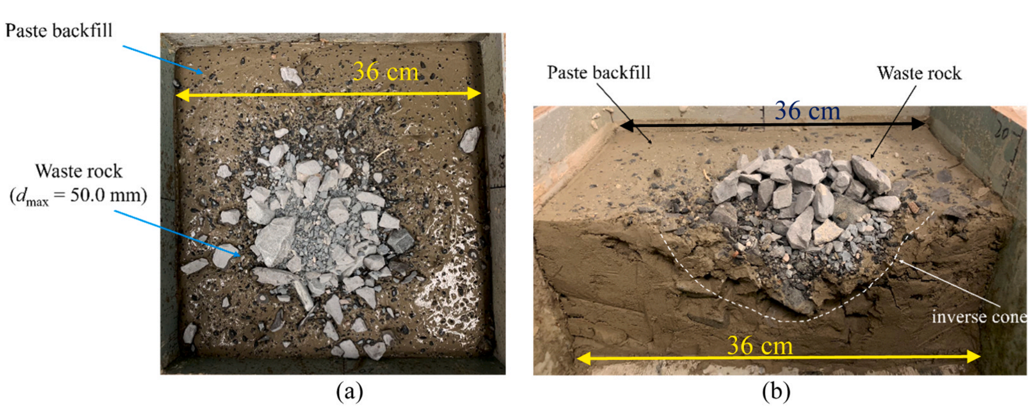

Fig. 8. A top view (a) and a cut view (b) of the mixing state of the dumped *WR* with a d_{max} of 50 mm and a total mass of 4441 g onto the PB at a dumping height of 75 cm.

Table 1
Material parameters used for the simulations of the tested *WR* and PB.

Material	Parameter	Value	Method
WR particles	Density (kg/m^3)	2760	Measured
	Young's modulus (GPa)	46.8	Measured[1]
	Poisson's ratio	0.19	Measured[1]
Particle to particle interaction of *WR*	Restitution coefficient	0.79	Measured[2]
	Static friction coefficient	0.466	Measured[2]
	Rolling resistance coefficient	0.15	Calibrated
PB	Yield stress (Pa)	136	Measured[3]
	Viscosity (Pa·s)	0.7	Calibrated[3]

Note: [1] measured by Major and Knupp [34] for the same *WR*; [2] measured by Sandeep et al. [35]; [3] measured and calibrated by Zhang and Li [30].

4. Discussion

The natural mixing behavior of *WR* and PB was investigated through a series of laboratory tests at multiple scales, complemented by predictive numerical simulations. All numerical results presented in this study are true predictions, as the model parameters, either experimentally measured or obtained through numerical calibration in Part I and Zhang and Li [30], were used without any further adjustment.

Good agreement was achieved between experimental and numerical results for the case involving *WR* with d_{max} of 5 mm. For the case with d_{max} = 2 mm, the model accurately predicted the unmixed mass of *WR* but significantly overestimated the mixed portion. Conversely, for d_{max} = 50 mm, the model closely predicted the mixed mass but largely overestimated the unmixed portion. These discrepancies for the 2 and 50 mm cases highlight a need for further investigation. In particular,

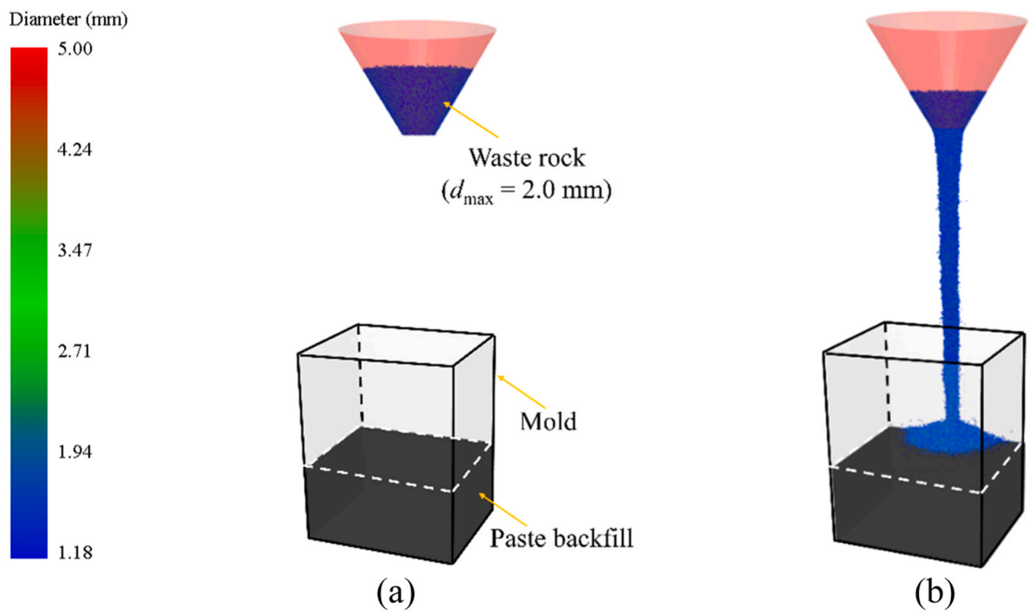

Fig. 9. Numerical model built with EDEM for predicting the test results of pouring *WR* with a d_{max} of 2.0 mm and a mass of 400 g onto the PB at a dumping height of 40 cm: (a) generation of *WR* particles; (b) pouring *WR* on the PB.

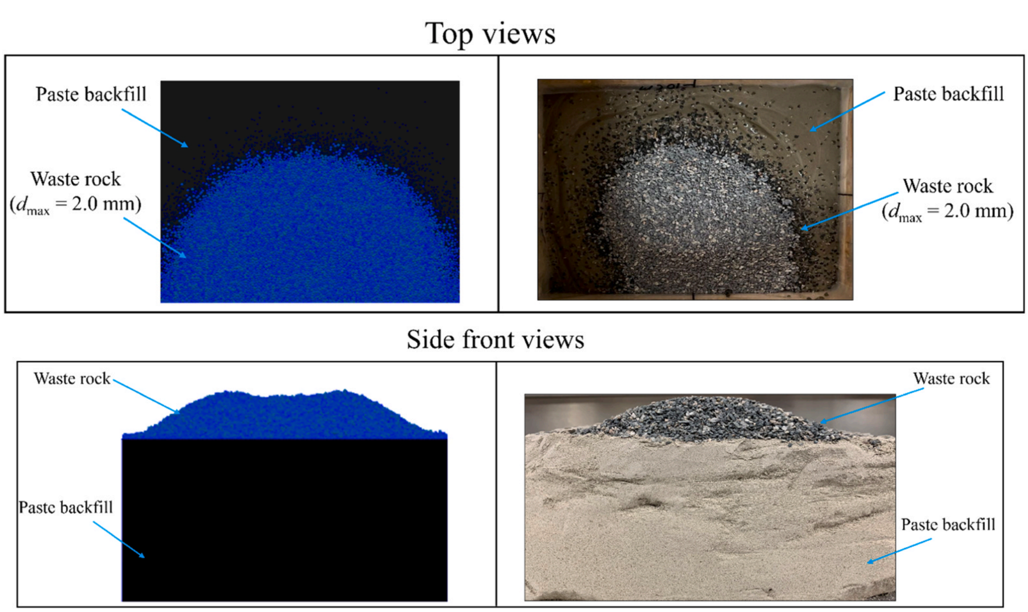

Fig. 10. Mixing state between the PB and the dumped *WR* with a d_{max} of 2.0 mm and a mass of 400 g at a dumping height of 40 cm, obtained by numerical predictions (left) and laboratory tests (right).

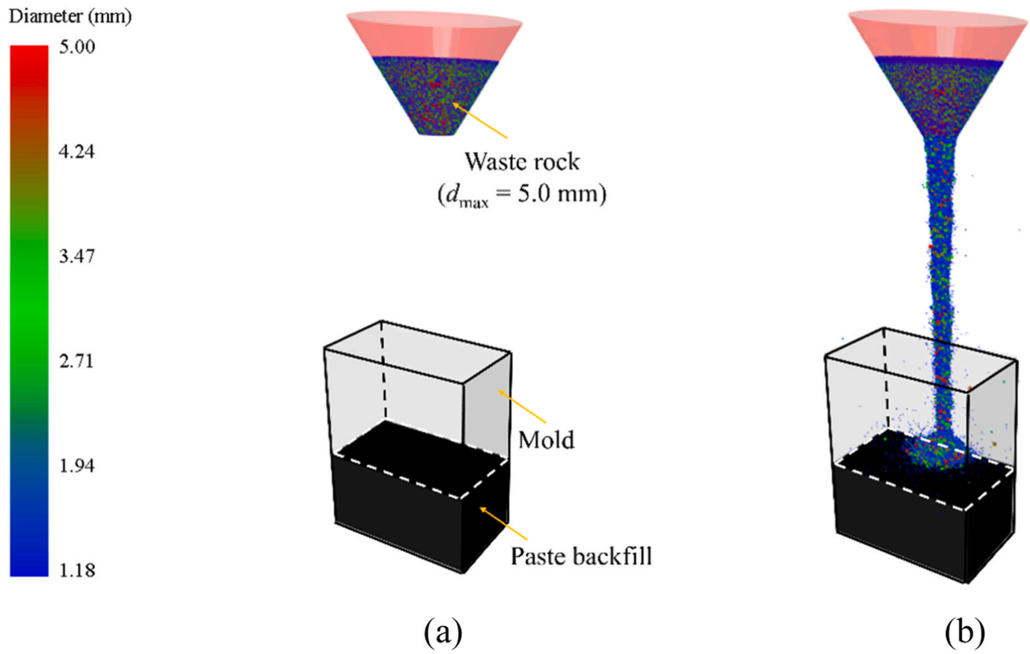

Fig. 11. Numerical model built with EDEM for predicting the test results of pouring *WR* with a d_{max} of 5.0 mm and a mass of 1400 g onto the PB at a dumping height of 40 cm: (a) generation of *WR* particles; (b) pouring *WR* on the PB.

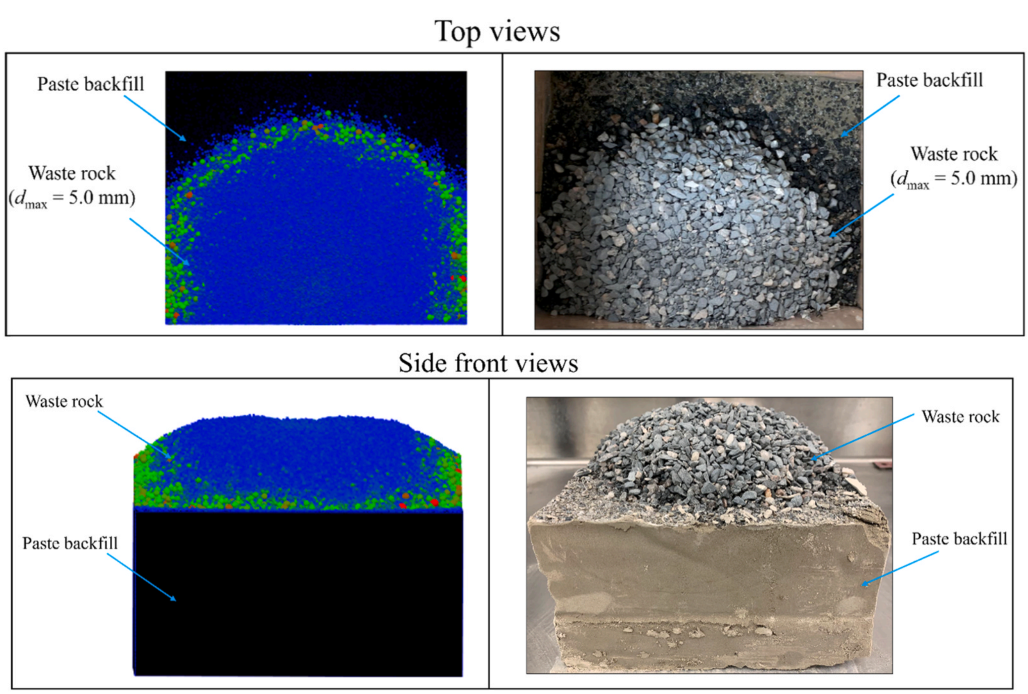

Fig. 12. Mixing state between the PB and the dumped *WR* with a d_{max} of 5.0 mm and a mass of 1400 g at a dumping height of 40 cm, obtained by numerical predictions (left) and laboratory tests (right).

questions arise regarding the reliability of the numerical model, the laboratory test procedures, or potentially both.

In the small-scale tests, *WR* was poured using a funnel along the sidewall at a specified dumping height. However, during the actual dumping process, deviation in the funnel's position and height may have occurred. As illustrated in Fig. 15, if the funnel tip shifted toward the center of the mold, a larger portion of *WR* could have penetrated and mixed with the PB than initially intended. Alternatively, when the funnel was too close to the sidewall, some *WR* particles may have fallen outside the box. In both scenarios, the actual experimental conditions derived from the idealized configuration represented in the numerical models (e.g., Figs. 9b and 11b), potentially contributing to the observed differences between the predicted and measured results.

For the large-scale test, it was readily observed that the lifting of the wooden decline and the dumping of the *WR* could easily deviate from the intended position and dumping height, as illustrated in Fig. 5. Additionally, the loss of *WR* particles falling outside the box was not considered. These factors suggest that several physical aspects were not accurately replicated in the numerical model. Consequently, the numerical simulation shown in Fig. 13 does not faithfully represent the

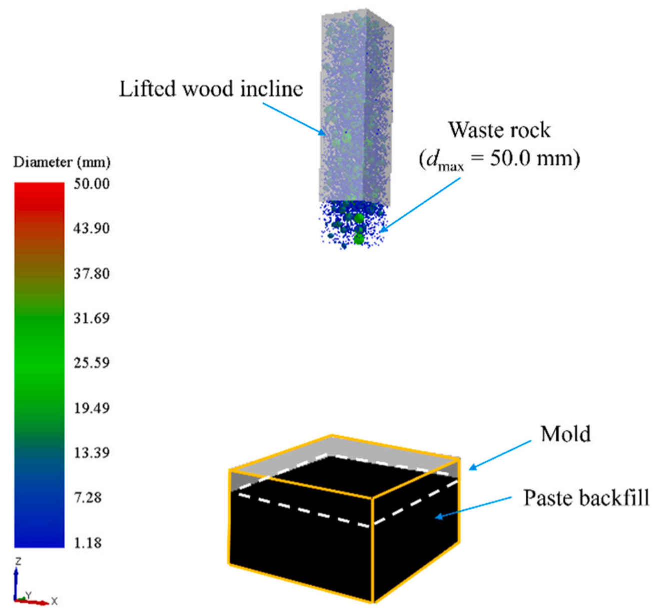

Fig. 13. Numerical model built with EDEM for predicting the large-scale test results of pouring *WR* with a d_{max} of 50.0 mm and a mass of 4441 g onto the PB at a dumping height of 75 cm.

physical conditions of the experimental setup shown in Fig. 5.

Given this discrepancy, the observed difference between experimental measurements and the numerical predictions should not be surprising. To address this, more controlled laboratory testing and improved numerical models that account for previously neglected physical variables are necessary.

These findings reinforce an important point: numerical modeling can be a powerful tool when used appropriated. However, in case of poor agreement between simulations and experimental data, it is essential to carefully examine the source of discrepancy, whether in the physical experiment, the numerical model, or both, instead of arbitrarily adjusting model parameters to force a better fit.

It is, of course, premature to attribute the poor agreements solely to experimental errors. Several limitations within the numerical model may also contribute to the discrepancies. For example, in the f-EDEM model developed by Zhang and Li [30], the effects of PB on *WR* particles were considered through vertical buoyance and drag forces, assuming that the PB remains static throughout the simulation. This simplification likely underrepresents the actual behavior of the fluid. In practice, the impact of dumped *WR* can induce dynamic responses in the PB, including splashing, lateral displacement, and fluid flow between particles; all of which were neglected in the current model.

Another unmodeled factor is the spatial variation of density and viscosity within the PB. In reality, tailings in PB tend to settle over time, resulting in lower density and viscosity at the top and higher values at the bottom. This stratification was not incorporated into the simulation.

In addition, another potential contributor to the discrepancy lies in the stochastic nature of the discrete element method. Particle generation (e.g., positions and number) varies between simulations, meaning results can differ significantly from one run to another. This variability highlights the importance of performing multiple runs to increase confidence in the numerical results, as demonstrated in Zhang and Li [30].

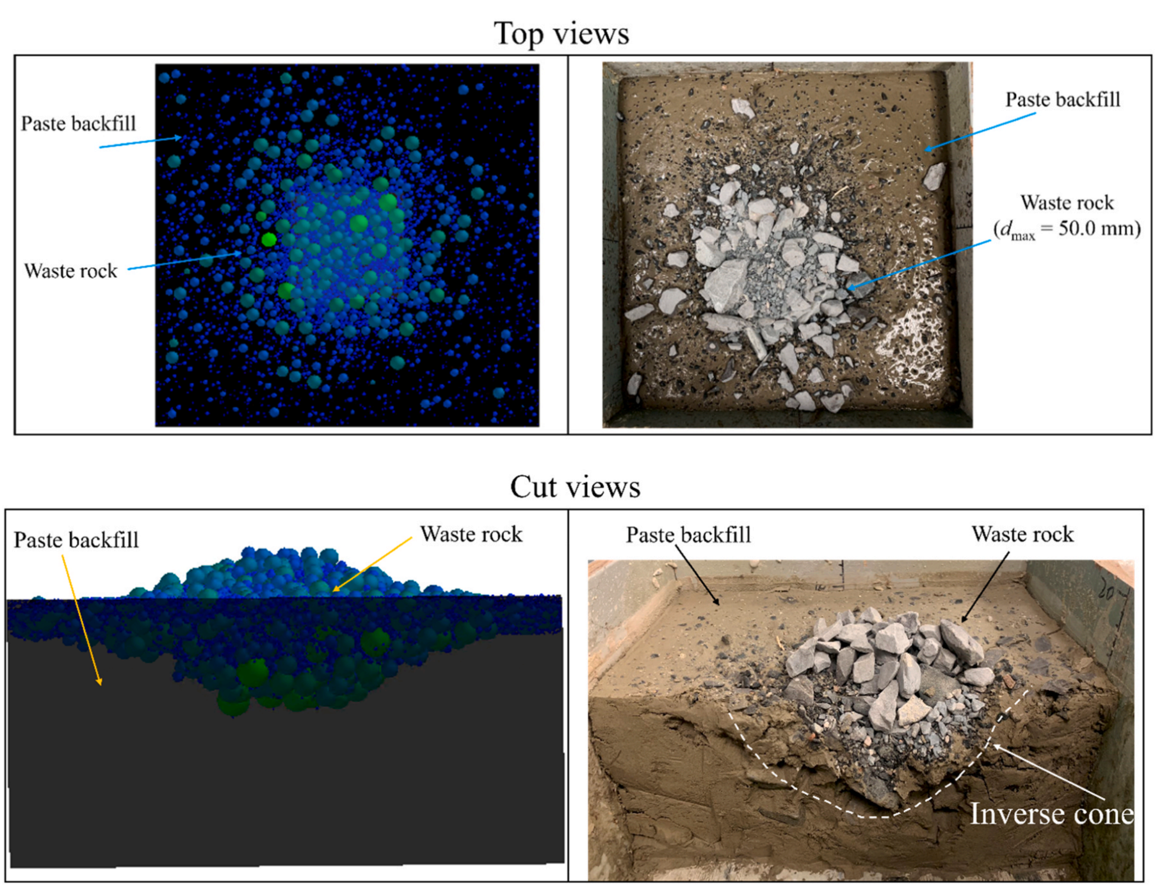

Fig. 14. Mixing state between the PB and the dumped *WR* with a d_{max} of 50.0 mm and a mass of 4441 g at a dumping height of 75 cm, obtained by numerical predictions (left) and laboratory tests (right).

Table 2
Measured and numerical predicted mixed and unmixed masses of dumped W*R* in PB.

d_{max} (mm)	Experiments		Numerical prediction	
	Mixed mass (g)	Unmixed mass (g)	Mixed mass (g)	Unmixed mass (g)
2	35.3 (measured)	364.7 (estimated)	59.46	340.54
5	193 (estimated)	1207 (measured)	131.08	1268.90
50	3996.5 (estimated)	444.5 (measured)	3537.66	903.34

It is also worth noting that all model parameters in Table 1 were either experimentally measured or obtained through numerical calibration, except for the restitution coefficient between rock-rock particles. This parameter was adopted from Sandeep et al. [35], and its suitability for use with W*R* particles remains uncertain.

These analyses clearly show that both the experimental setup and the in numerical model have limitations that can partly explain the observed discrepancies. However, they also point to a clear path forward for improving both approaches. The utility of numerical modeling is again demonstrated, particularly as a predictive tool when used with a sound understanding of its limitations.

Fig. 15. A picture taken during the dumping of W*R* onto the PB for small-scale tests.

A major limitation of the current numerical model lies in its inability to directly simulate PB particles directly, due to their extremely small sizes and large quantity. As a result, the model cannot yet fully capture or quantify the quality of mixing between the W*R* and PB. Furthermore, the current model is not capable of simulating the penetration or flow of PB slurry into fractures or joints within surrounding rock mass, nor its movement through previously placed W*R* on the stope floor prior to PB placement. Addressing these limitations will require further development to enhance the model's capability and improve its representativeness in more complex field conditions.

In this study, the numerical simulations were conducted for the dumping of W*R* into uncemented PB with a solids content of 75% by mass. Future research should include experimental and numerical investigations across a broader range of solids contents. Moreover, the current maximum tested d_{max} value of 5 cm is still much smaller than the typical value of approximately 60 cm for underground W*R*. Therefore, large-scale laboratory tests using W*R* with higher d_{max} values are necessary to determine the limits of validity of the numerical model.

Ultimately, the predictive capability of the model for simulating the natural mixing behavior of dumped W*R* and PB should be tested under realistic field conditions in an operating underground mine.

Finally, further studies are required to evaluate the natural mixing behavior of W*R* not only with uncemented PB but also with cemented PB. Future investigation should explore a wide range of influencing factors, including the dumping location of the W*R*, the use of multiple dumping points, the multi-phase backfilling operations, the presence of water or mud within the W*R*, the effects of blasting induced vibrations, and the inclination of stope walls.

Once the degree of mixture is evaluated, the strength of the fill mass can be assed as a function of this degree of mixing, allowing the determination of its spatial strength distribution. With this information, the stability of the fill mass formed by the natural mixture of dumped W*R* and PB, under side or base exposure, can then be thoroughly evaluated.

5. Conclusions

The natural mixing behavior of dumped W*R* and a PB was investigated through a combination of laboratory experiments and numerical modeling. Laboratory tests were conducted at multiple scales, ranging from small-scale setups using W*R* with smaller maximum particle size (d_{max}) to large-scale tests involving coarser W*R* with larger d_{max}. The validated and calibrated numerical model developed in Part I of the study was applied, without further adjustment, to predict the outcome of these physical tests.

The results show that the numerical model was able to accurately predict several aspects of the mixing behavior, ranging from small-scale tests with fine W*R* and moderate dumping height to large-scale tests involving coarse W*R* and greater dumping height. These successful predictions partly confirm the model's applicability and predictive capability across a range of conditions. The model holds promise for predicting the natural mixing behavior between PB and dumped W*R* with larger d_{max} in a large-scale or even field-scale scenario.

Notable discrepancies between some experimental results and numerical predictions were also observed. These inconsistencies proved valuable, as they revealed limitations in both the laboratory testing setup and the numerical model. Issues such as variation in duping position, uncontrolled dumping height, and neglected physical behavior (e.g. splash, or flow of PB) were identified in the experimental setup. Similarly, simplifying assumptions and constraints within the numerical model, including its treatment of PB dynamic and the stochastic nature of DEM simulations, were recognized as source of potential error.

These findings help to define the direction for future improvement in both experimental design and numerical modeling. The study also highlights the importance of using numerical modeling thoughtfully: understanding its assumptions and limitations and resisting the temptation to arbitrarily adjust model parameters to force agreement with test data.

This work underscores the significant value of numerical modeling as a predictive tool for evaluating the natural mixing behavior between *WR* and PB in underground mining applications, while also offering a roadmap for further development and validation.

CRediT authorship contribution statement

Yuyu Zhang: Writing – original draft, Visualization, Validation, Software, Methodology, Investigation, Formal analysis, Data curation, Conceptualization. **Li Li:** Writing – review & editing, Supervision, Resources, Project administration, Methodology, Investigation, Funding acquisition, Formal analysis. **Louis-Philippe Gélinas:** Writing – review & editing, Resources, Formal analysis. **Serge Ouellet:** Writing – review & editing, Resources, Formal analysis.

Declaration of Competing Interest

The authors declare that they have no known competing financial interests or personal relationships that could have appeared to influence the work reported in this paper. The author Li Li is a member of the editorial board for Deep Resources Engineering and was not involved in the editorial review or the decision to publish this article.

Acknowledgments

The authors acknowledge the financial support from the Natural Sciences and Engineering Research Council of Canada (RGPIN-2024–06859 and ALLRP 580767–22), and industrial partners of the Research Institute on Mines and the Environment (RIME UQAT–Polytechnique; http://rime-irme.ca). The anonymous reviewers are also gratefully acknowledged for their constructive comments and suggestions, which are very helpful for improving the quality and coherences of the manuscript.

Data availability statement

All data included in this study are available upon reasonable request by contact with the corresponding author.

References

[1] C. Lee, F.Q. Gu, An examination of improvements in co-disposal of waste rock with backfill, in: A. Wu, R. Jewell (Eds.), Paste 2017: Proceedings of the 20th International Seminar on Paste and Thickened Tailings, University of Science and Technology Beijing, Beijing, 2017, pp. 338–345.
[2] I. Hane, T. Belem, M. Benzaazoua, et al., Laboratory characterization of cemented tailings paste containing crushed waste rocks for improved compressive strength development, Geotech. Geol. Eng. 35 (2) (2017) 645–662.
[3] H.F. Qiu, F.S. Zhang, L. Liu, et al., Influencing factors on strength of waste rock tailing cemented backfill, Geofluids 2020 (2020) 8847623.
[4] H.F. Qiu, F.S. Zhang, W.B. Sun, et al., Experimental study on strength and permeability characteristics of cemented rock-tailings backfill, Front. Earth Sci. 10 (2022) 802818.
[5] F. Hassani, J. Archibald, Mine backfill (CD-ROM), CIM, Montreal, QC, Canada, 1998.
[6] Y. Potvin, E. Thomas, A. Fourie. Handbook on mine fill, Australian Centre of Geomechanics, University of Western Australia, Nedlands, Australia, 2005.
[7] R.J. Mitchell, R.S. Olsen, J.D. Smith, Model studies on cemented tailings used in mine backfill, Can. Geotech. J. 19 (1) (1982) 14–28.
[8] R.J. Mitchell, Sill mat evaluation using centrifuge models, Min. Sci. Technol. 13 (3) (1991) 301–313.
[9] K. le Roux, W.F. Bawden, M.F. Grabinsky, Field properties of cemented paste backfill at the Golden Giant mine, Min. Technol.: Trans. Inst. Min. Metall. 114 (2) (2005) 65–80.
[10] M. Fall, M. Benzaazoua, S. Ouellet, Experimental characterization of the influence of tailings fineness and density on the quality of cemented paste backfill, Miner. Eng. 18 (1) (2005) 41–44.
[11] A. Kesimal, E. Yilmaz, B. Ercikdi, et al., Effect of properties of tailings and binder on the short- and long-term strength and stability of cemented paste backfill, Mater. Lett. 59 (28) (2005) 3703–3709.
[12] T. Belem, M. Benzaazoua, Design and application of underground mine paste backfill technology, Geotech. Geol. Eng. 26 (2) (2008) 147–174.
[13] M. Fall, M. Pokharel, Coupled effects of sulphate and temperature on the strength development of cemented tailings backfills: Portland cement-paste backfill, Cem. Concr. Compos. 32 (10) (2010) 819–828.
[14] M. Helinski, M. Fahey, A. Fourie, Behavior of cemented paste backfill in two mine stopes: Measurements and modeling, J. Geotech. Geoenviron. Eng. 137 (2) (2011) 171–182.
[15] B.D. Thompson, W.F. Bawden, M.W. Grabinsky, In situ measurements of cemented paste backfill at the Cayeli Mine, Can. Geotech. J. 49 (7) (2012) 755–772.
[16] L. Cui, M. Fall, A coupled thermo-hydro-mechanical-chemical model for underground cemented tailings backfill, Tunn. Undergr. Space Technol. 50 (2015) 396–414.
[17] L. Cui, M. Fall, Multiphysics model for consolidation behavior of cemented paste backfill, Int. J. Geomech. 17 (3) (2017) 04016077.
[18] C. Caceres, R. Moffat, R. Pakalnis, Evaluation of flexural failure of sill mats using classical beam theory and numerical models, Int. J. Rock Mech. Min. Sci. 99 (2017) 21–27.
[19] P.Y. Yang, L. Li, M. Aubertin, et al., Stability analyses of waste rock barricades designed to retain paste backfill, Int. J. Geomech. 17 (3) (2017) 04016079.
[20] M.J. Raffaldi, J.B. Seymour, J. Richardson, et al., Cemented paste backfill geomechanics at a narrow-vein underhand cut-and-fill mine, Rock Mech. Rock Eng. 52 (2019) 4925–4940.
[21] Y. Wang, Y.S. Cao, L. Cui, et al., Effect of external sulfate attack on the mechanical behavior of cemented paste backfill, Constr. Build. Mater. 263 (2020) 120968.
[22] Y.L. Zhai, P.Y. Yang, L. Li, Analytical solutions for the design of shotcreted waste rock barricades to retain slurried paste backfill, Constr. Build. Mater. 307 (2021) 124626.
[23] G.D. Lu, A.P.S. Selvadurai, M.A. Meguid, Analytical solution to non-isothermal pore-pressure evolution in hydrating minefill, Can. Geotech. J. 61 (12) (2024) 2722–2734.
[24] C. Lee, P. Gillot, Case study – a high strength paste aggregate backfill at Randgold's Loulo mine in Mali, in: Y. Potvin, T. Grice (Eds.), Mine Fill 2014: Proceedings of the Eleventh International Symposium on Mining with Backfill, Australian Centre for Geomechanics, Perth, 2014, pp. 231–242.
[25] G. Baldwin, A. Grice, Engineering the new Olympic Dam backfill system, Proc. Mass. (2000) 705–711.
[26] W. Sun, H.J. Wang, K.P. Hou, Control of waste rock-tailings paste backfill for active mining subsidence areas, J. Clean. Prod. 171 (2018) 567–579.
[27] K. Kugan, S. Ian, A non-segregating rocky paste fill (RPF) produced by co- disposal of cemented de-slimed tailings slurry and graded rockfill, Soc. Min. Metall. Explor. (2001) 1–15.
[28] Y.Y. Zhang, L. Li, Experimental study on the natural mixing behaviour of waste rocks poured in a paste backfill, Int. J. Min. Reclam. Environ. 37 (10) (2023) 953–977.
[29] L. Li, Special issue on numerical modeling in civil and mining geotechnical engineering, Processes 10 (8) (2022) 1571.
[30] Y.Y. Zhang, L. Li, Introduction and implementation of fluid forces in a DEM code for simulating particle settlement in fluids, Powder Technol. 433 (2024) 119238.
[31] Y.Y. Zhang, L. Li, Optimization of discrete element method model to obtain stable and reliable numerical results of mechanical response of granular materials, Minerals 14 (8) (2024) 758.
[32] A. Deiminiat, L. Li, Experimental study on the reliability of scaling down techniques used in direct shear tests to determine the shear strength of rockfill and waste rocks, CivilEng 3 (1) (2022) 35–50.
[33] Altair EDEM, Altair EDEM 2022.2 Release Notes, Altair Engineering Inc, 2022.
[34] G. Major, R. Knupp, Report on feasibility-level pit slope design criteria Osisko Canadian Malartic project. Golder Associates Inc. (2008) ⟨https://archives.bape.gouv.qc.ca/sections/mandats/Mines_Malartic/documents/DA27.pdf⟩ (accessed 5 Oct 2025).
[35] C.S. Sandeep, K. Senetakis, D. Cheung, et al., Experimental study on the coefficient of restitution of grain against block interfaces for natural and engineered materials, Can. Geotech. J. 58 (1) (2021) 35–48.

Dr. Li Li is a registered engineer with Ordre des ingénieurs du Québec (OIQ) and a professor of mining engineering at Polytechnique Montreal. He was the Head of Mining Engineering Program at Polytechnique Montreal between 2020 and 2023. He serves the Research Institute on Mines and Environment (RIME) UQAT-Polytechnique as a Scientific Director since May 2023 (https://irme.ca/en/rime/). He has more than twenty-year experience in geomechanical and geotechnical engineering. Over the past decade, his research has mainly focused on underground mining with backfill (stress estimation in backfilled stopes, sizing barricades made of waste rock, assessing required strength of backfill with side- or base- exposure).